A Reduced-Complexity, Highly Power-/Bandwidth-Efficient Coded Feher-Patented Quadrature-Phase-Shift-Keying System with Iterative Decoding

M. K. Simon[1] and D. Divsalar[1]

Based on a representation of Feher-patented quadrature-phase-shift keying (FQPSK) as a trellis-coded modulation, this article investigates the potential improvement in power efficiency obtained from the application of simple (a small number of states) outer codes to form a concatenated coding arrangement with iterative decoding. Several possible configurations for the concatenation are suggested, and specific numerical results are presented for one of these in order to demonstrate the large coding gains that are achievable even when using a reduced-complexity FQPSK receiver. The end result of these investigations is a system that has application in scenarios requiring a high degree of both power and bandwidth efficiency.

I. Introduction

Feher-patented quadrature-phase-shift keying (FQPSK) [1–5] whose generic form finds its roots in cross-correlated phase-shift keying (XPSK) [6] is a highly spectral efficient modulation that is derived from staggered quadrature overlapped raised-cosine (SQORC) [7] modulation but unlike the latter maintains a nearly constant envelope[2] by manipulating the pulse shapes of the in-phase (I) and quadrature (Q) baseband signals via a cross-correlation mapping. To achieve additional spectral efficiency and true constant envelope, filtered (with a proprietary design) and hard-limited variants of FQPSK referred to as FQPSK-B [1,8] have been implemented in commercial hardware, and they achieve bandwidth efficiencies comparable to Gaussian minimum-shift keying (GMSK) [9], a modulation used in the Global System for Mobile (GSM) cellular mobile communication system [10] currently deployed in Europe. Because of its demonstrated ability to achieve high data rates (FQPSK-B modems operating at a data rate of 20 Mb/s are currently available as an off-the-shelf product from several commercial vendors), FQPSK-B has been recommended for adoption as a standard by the Consultative Committee on Space Data Systems (CCSDS) and the Interrange Instrumentation Group (IRIG) [11]. FQPSK-B has also been adopted by the U.S. Department of Defense joint services Advanced Range Telemetry (ARTM)

[1] Communications Systems and Research Section.

[2] The maximum fluctuation in the envelope of the modulated signal is 0.18 dB.

The research described in this publication was carried out by the Jet Propulsion Laboratory, California Institute of Technology, under a contract with the National Aeronautics and Space Administration.

program as its Tier I modulation for missile, aircraft, and range applications to replace existing pulse code modulation/frequency modulation (PCM/FM).

As is true for most bandwidth-efficient modulation (BEM) schemes, the price paid for a high degree of spectral efficiency is a degradation in bit-error rate (BER) performance. FQPSK (or FQPSK-B) is no exception to this rule. Specifically, using the traditional (symbol-by-symbol detection) FQPSK receiver, the signal-to-noise ratio (SNR) degradation relative to the highly bandwidth inefficient binary-phase-shift keying (BPSK) is already 1.4 dB at a BER of 10^{-3}. Recently, a new interpretation of FQPSK as a cross-correlated, trellis-coded quadrature modulation (XTCQM) [12] was introduced in [13] and by virtue of replacing the traditional receiver with a trellis (Viterbi) demodulator allowed for the possibility of achieving a significant improvement in power efficiency. While the full benefit of the power efficiency improvement was obtained using the optimum receiver, i.e., one that implements a 16-state trellis [13], a reduced-complexity Viterbi receiver with only 2 states per I and Q channel has been shown [14] to yield FQPSK-B performance within a few tenths of a dB of the optimum one.

While the previous two contributions [13,14] are quite significant in their own right in both enhancing the BER performance and simplifying the receiver complexity, the desire to achieve additional power efficiency while at the same time maintaining the high degree of bandwidth efficiency inherent in the modulation motivated the authors to investigate the application of error-correction coding to FQPSK.[3] Here again, as in [14], the motivation was accompanied by the desire to maintain a simple receiver architecture. As such, we investigated the coupling (through an interleaver) of very simple short-constraint-length codes with the convolutional coding inherent in the FQPSK modulation itself [13] to determine how much further SNR improvement is achievable. This article reports the results of the somewhat dramatic findings of these investigations.

II. The Trellis-Coded Interpretation of FQPSK and its Reception

As implied above, in its generic (unfiltered) form, FQPSK is conceptually the same as XPSK introduced in 1983 by Kato and Feher [6]. This technique was in turn a modification of the previously introduced (by Feher et al. [15]) interference and jitter-free quadrature-phase-shift keying (IJF-QPSK) with the express purpose of reducing the 3-dB envelope fluctuation characteristic of IJF-QPSK to 0 dB (or as close to that as possible),[4] thus making it appear constant envelope. It is further noted that, using a constant waveshape for the even pulse and a sinusoidal waveshape for the odd pulse, which was the case considered in [6], IJF-QPSK becomes identical to the SQORC scheme introduced by Austin and Chang [7]. The means by which Kato and Feher achieved their 3-dB envelope reduction was the introduction of an intentional but controlled amount of cross-correlation between the I and Q channels. This cross-correlation operation was applied to the IJF-QPSK (SQORC) baseband signal prior to its modulation onto the I and Q carriers (see Fig. 1). Specifically, this operation was described by mapping in each *half* symbol the 16 possible combinations of I- and Q-channel waveforms present in the SQORC signal into a new[5] set of 16 waveform combinations chosen in such a way that the cross-correlator output is time continuous and has unit (normalized) envelope at all I and Q uniform sampling instants. By virtue of the fact that the cross-correlation mapping is based on a half-symbol characterization of the SQORC signal, there is no guarantee that the *slope* of the cross-correlator output waveform is continuous at the half-symbol transition points. In fact, it has been shown [13] that for a random data input sequence such a discontinuity in slope occurs one-quarter of the time.

---

[3] Needless to say, there is an inevitable bandwidth expansion that occurs proportional to the inverse of the code rate. The hope is to produce a coding (power) gain that more than compensates for this bandwidth expansion.

[4] The reduction of the envelope from 3 dB to 0 dB occurs only at the uniform sampling instants on the I and Q channels, i.e., in between these sampling instants, the envelope has a small amount of fluctuation, as previously stated. For this reason, XPSK (or FQPSK) is referred to as being "pseudo"—or "quasi"—constant envelope.

[5] Of the 16 possible cross-correlator output combinations, only 12 of them are in fact new, i.e., for 4 of the input I and Q combinations, the cross-correlator outputs the identical combination.

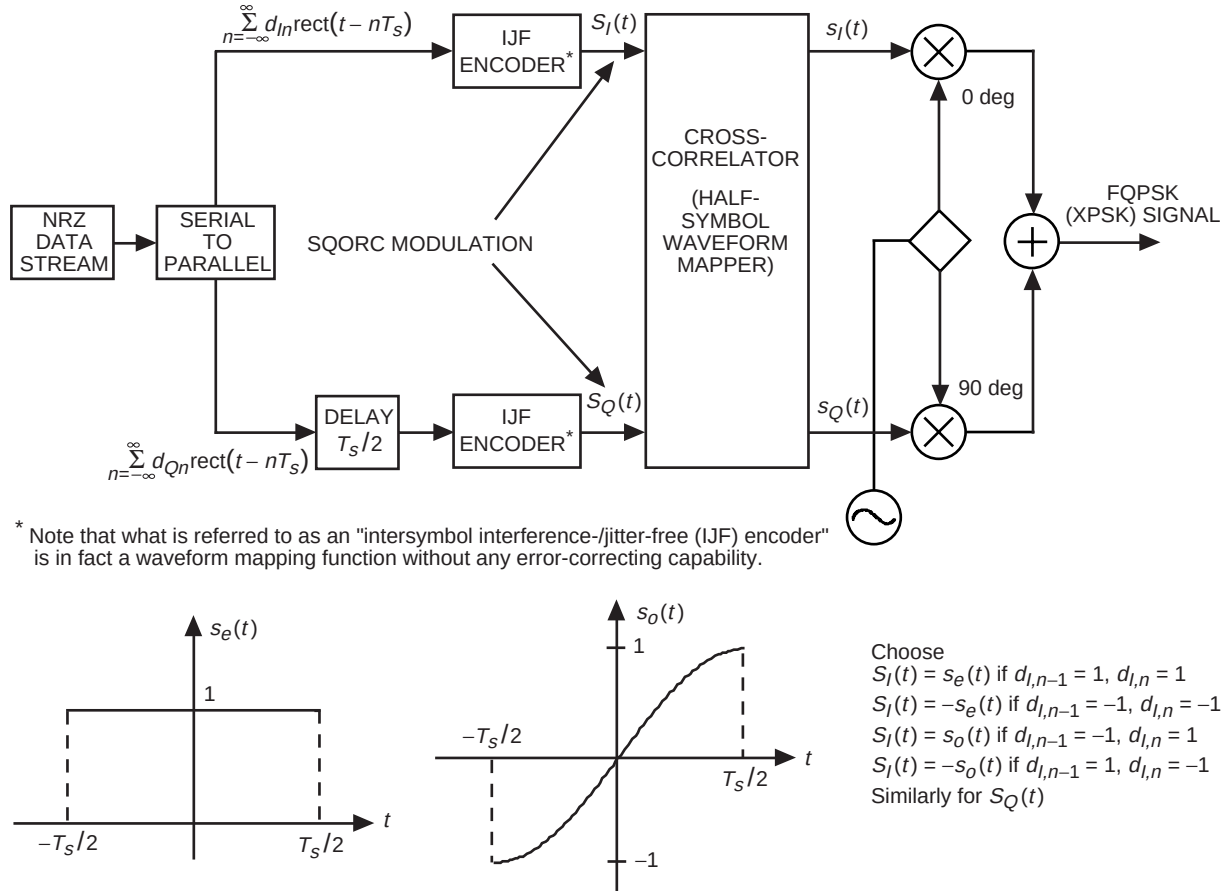

Fig. 1. Conceptual block diagram of FQPSK (XPSK).

By restructuring the cross-correlation mapping into a *symbol-by-symbol* (rather than *half-symbol-by-half-symbol*) representation as proposed in [13], the slope discontinuity referred to above is placed in evidence and at the same time suggests a means to eliminate it.[6] This representation also has the advantage that it can be described directly in terms of the data transitions on the I and Q channels and, thus, the combination of IJF encoder and cross-correlator in Fig. 1 can be replaced simply by a single modified cross-correlator (to be discussed shortly).

A further and more important advantage of the reformulation as a symbol-by-symbol mapping is the ability to design a receiver for FQPSK (or enhanced FQPSK) that specifically exploits the correlation introduced into the modulation scheme to significantly improve power efficiency or, equivalently, BER performance. Such a receiver that takes a form analogous to those used for trellis-coded modulations will yield significant performance improvement over receivers that employ symbol-by-symbol detection, thereby ignoring the inherent memory of the modulation.

Figure 2 is an illustration of the trellis-coded interpretation of FQPSK. The input data bit stream is split into time-aligned I and Q symbol streams, each at half the bit rate, i.e., $1/T_s = 1/2T_b$. Each of these symbol streams is passed through rate-1/3 convolutional encoders (note that the I- and Q-channel

[6] Since the rate at which the spectral side lobes of a modulation's power spectral density (PSD) roll off with frequency is related to the smoothness of the underlying waveforms, one would anticipate that elimination of the slope discontinuity would enhance spectral efficiency. Indeed, this has been shown to to be the case in [13] and results in what is referred to there as *enhanced* FQPSK.

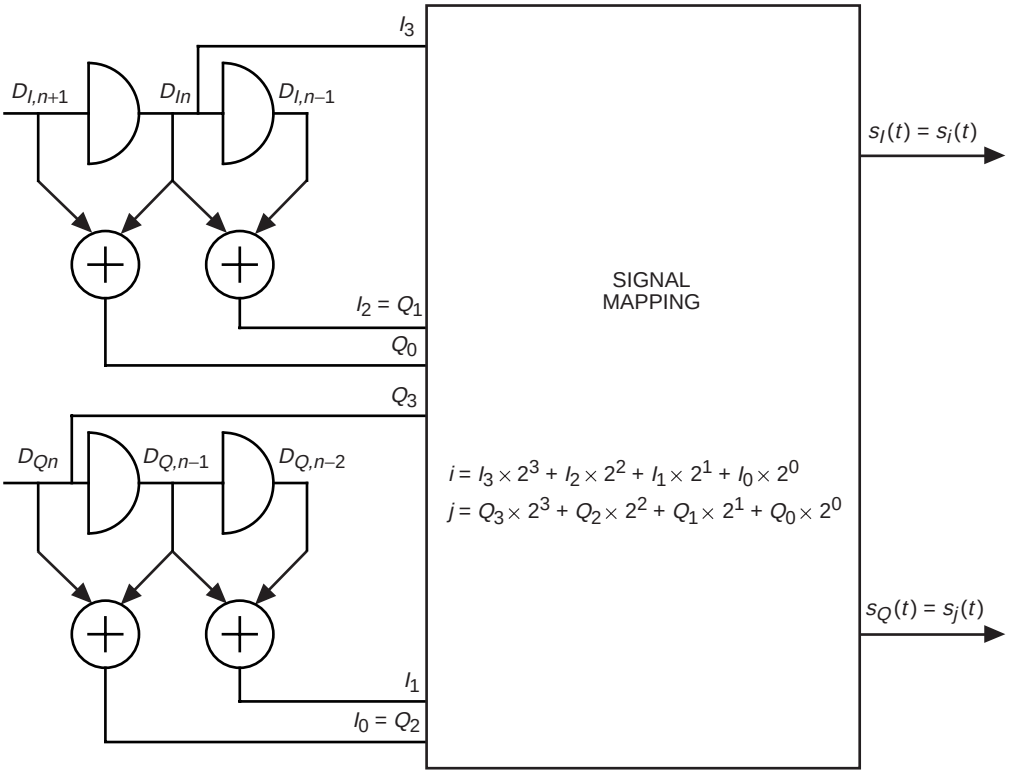

Fig. 2. Alternative implementation of FQPSK baseband signals.

encoders are different). The output bits of these encoders can be considered to be grouped into three categories—those that influence only the choice of the signal in the same channel, those that influence only the choice of the signal in the other channel, and those that influence the choice of the signal in both channels (hence the notion of cross-correlation mapping). For example, of the 3 bits that emanate from the I encoder in Fig. 2, I_3 is used to determine the signal transmitted on the I channel, Q_0 is used to determine the signal transmitted on the Q channel, and $I_2 = Q_1$ is used to determine both the signals transmitted on the I and Q channels. Letting d_{In} and d_{Qn}, respectively, denote the $(+1, -1)$ I and Q data symbols in the nth transmission interval and $D_{In} \triangleq (1 - d_{In})/2$ and $D_{Qn} \triangleq (1 - d_{Qn})/2$ their (0,1) equivalents, then the mappings appropriate to the I and Q encoders of Fig. 2 are

$$\left.\begin{aligned} I_0 &= D_{Qn} \oplus D_{Q,n-1}, & Q_0 &= D_{I,n+1} \oplus D_{In} \\ I_1 &= D_{Q,n-1} \oplus D_{Q,n-2}, & Q_1 &= D_{In} \oplus D_{I,n-1} = I_2 \\ I_2 &= D_{In} \oplus D_{I,n-1}, & Q_2 &= D_{Qn} \oplus D_{Q,n-1} = I_0 \\ I_3 &= D_{In}, & Q_3 &= D_{Qn} \end{aligned}\right\} \tag{1}$$

Corresponding to the four I-channel coded bits (two from the I-encoder output and two from the Q-encoder output) and likewise for the four Q-channel coded bits, a pair of binary coded decimal (BCD) indices, (i, j), is defined in accordance with

$$\left.\begin{aligned} i &= I_3 \times 2^3 + I_2 \times 2^2 + I_1 \times 2^1 + I_0 \times 2^0 \\ j &= Q_3 \times 2^3 + Q_2 \times 2^2 + Q_1 \times 2^1 + Q_0 \times 2^0 \end{aligned}\right\} \tag{2}$$

These indices range over the set of integers between 0 and 15 and are used to select the baseband signals $s_i(t)$ and $s_j(t)$ to be transmitted on the I and Q channels, respectively. The set of waveforms (of duration T_s) from which $s_i(t)$ and $s_j(t)$ are selected in each transmission (symbol) interval is illustrated in Fig. 3 and defined as follows:

$$\left.\begin{aligned}
s_0(t) &= A, && -\frac{T_s}{2} \le t \le \frac{T_s}{2}, && s_8(t) = -s_0(t) \\
s_1(t) &= \begin{cases} A, & -\frac{T_s}{2} \le t \le 0, \\ 1-(1-A)\cos^2\frac{\pi t}{T_s}, & 0 \le t \le \frac{T_s}{2}, \end{cases} && && s_9(t) = -s_1(t) \\
s_2(t) &= \begin{cases} 1-(1-A)\cos^2\frac{\pi t}{T_s}, & -\frac{T_s}{2} \le t \le 0, \\ A, & 0 \le t \le \frac{T_s}{2}, \end{cases} && && s_{10}(t) = -s_2(t) \\
s_3(t) &= 1-(1-A)\cos^2\frac{\pi t}{T_s}, && -\frac{T_s}{2} \le t \le \frac{T_s}{2}, && s_{11}(t) = -s_3(t) \\
s_4(t) &= A\sin\frac{\pi t}{T_s}, && -\frac{T_s}{2} \le t \le \frac{T_s}{2}, && s_{12}(t) = -s_4(t) \\
s_5(t) &= \begin{cases} A\sin\frac{\pi t}{T_s}, & -\frac{T_s}{2} \le t \le 0, \\ \sin\frac{\pi t}{T_s}, & 0 \le t \le \frac{T_s}{2}, \end{cases} && && s_{13}(t) = -s_5(t) \\
s_6(t) &= \begin{cases} \sin\frac{\pi t}{T_s}, & -\frac{T_s}{2} \le t \le 0, \\ A\sin\frac{\pi t}{T_s}, & 0 \le t \le \frac{T_s}{2}, \end{cases} && && s_{14}(t) = -s_6(t) \\
s_7(t) &= \sin\frac{\pi t}{T_s}, && -\frac{T_s}{2} \le t \le \frac{T_s}{2}, && s_{15}(t) = -s_7(t)
\end{aligned}\right\} \tag{3}$$

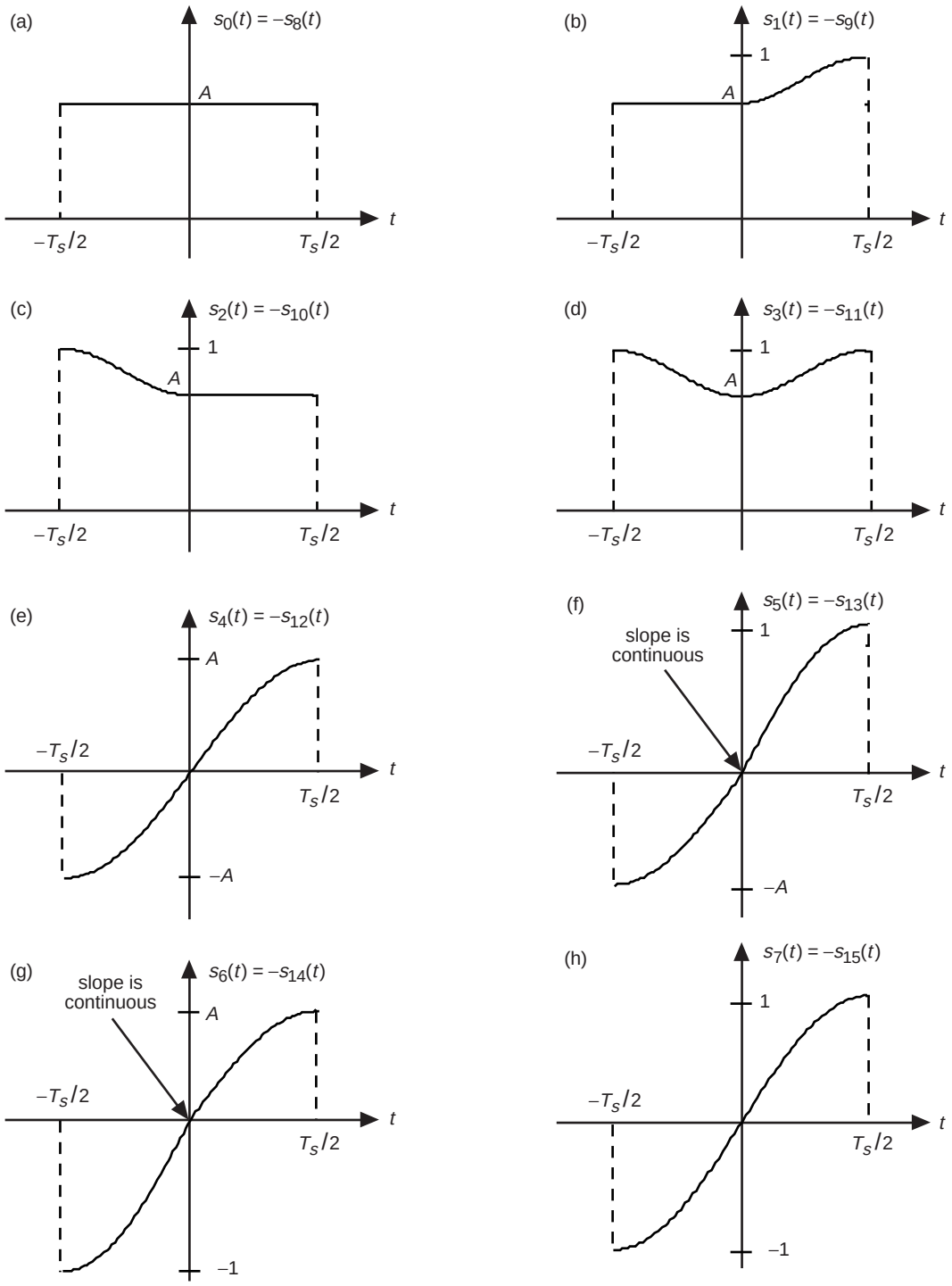

Fig. 3. FQPSK full-symbol waveforms (A = $1/\sqrt{2}$ for "constant envelope"): (a) $s_0(t) = -s_8(t)$ vs t, (b) $s_1(t) = -s_9(t)$ vs t, (c) $s_2(t) = -s_{10}(t)$ vs t, (d) $s_3(t) = -s_{11}(t)$ vs t, (e) $s_4(t) = -s_{12}(t)$ vs t, (f) $s_5(t) = -s_{13}(t)$ vs t, (g) $s_6(t) = -s_{14}(t)$ vs t, and (h) $s_7(t) = -s_{15}(t)$ vs t.

Note that for any value of A other then unity, e.g., $A = 1/\sqrt{2}$ (the value suggested in [6] as leading to minimum envelope fluctuation), $s_5(t)$ and $s_6(t)$ as well as their negatives, $s_{13}(t)$ and $s_{14}(t)$, will have discontinuous slopes at their midpoints (i.e., at $t = 0$), whereas the remaining 12 waveforms all have continuous slopes throughout their defining intervals. This confirms statements made earlier and also suggests the further enhancement in spectral efficiency discussed in [13] obtained by redefining $s_5(t), s_6(t), s_{13}(t), s_{14}(t)$ so as not to have a midpoint slope discontinuity.[7] Also, all 16 waveforms in Eq. (3) have zero slopes at their end points and, thus, concatenation of any pair of these as results when data are sequentially transmitted will similarly not result in a slope discontinuity.

Finally, the I and Q baseband signals, $s_I(t)$ and $s_Q(t)$, are offset (by half a symbol) relative to one another, modulated onto quadrature carriers, and then summed for transmission over the RF channel.

The above trellis-coded characterization of FQPSK is in principle an M-ary signaling scheme, i.e., a given pair of I and Q data symbols results in the transmission of a given pair of I and Q waveforms in each signaling interval. However, because of the presence of the I and Q encoders and the cross-correlation mapping, restrictions are placed on the allowable sequences of waveforms that can be transmitted in each of these channels, e.g., the I- and Q-waveform sequences will always be continuous. It is these restrictions on the transitional behavior of the transmitted signal that result in the narrow spectrum characteristic of FQPSK. More important, however, is the fact that the trellis-coded structure of the transmitter suggests that the optimum receiver of FQPSK should be a form of trellis demodulator. In [13] it was shown that such an optimum receiver (see Fig. 4) consists of a bank of 16 energy-biased matched filters[8] (8 in each of the I and Q channels) followed by a 16-state trellis demodulator. The simulated BER performance of FQPSK using the receiver in Fig. 4 was presented in [13] and is illustrated here in Fig. 5 along with that obtained by using a conventional offset QPSK (OQPSK) receiver. Also shown for purposes of comparison is the BER performance of conventional uncoded QPSK.

In a desire to reduce the complexity of the 16-state receiver of Fig. 4 with the hope of not sacrificing significant power efficiency, two suboptimum configurations were considered. The first and least complex is the average matched-filter receiver [13] that replaces the bank of 16 matched filters by a single filter matched to the average of the 16 waveforms in Fig. 3, followed by symbol-by-symbol detection. Unfortunately, this memoryless receiver gives a performance only slightly better than that obtained from the conventional OQPSK receiver, which is also memoryless.

In an attempt to bridge the gap between the 16-state optimum receiver and the oversimplified average matched-filter receiver, a reduced-complexity FQPSK Viterbi receiver was considered in [14], based on the following considerations. Recognizing the similarity in the shape properties (e.g., "odd" versus "even," "flat" versus "sinusoidal") of certain members of the waveform set in Fig. 3, the 16 waveforms of this set were separated into four different groups (in reality two groups and their negatives) as follows: $s_0(t)$ through $s_3(t)$, $s_4(t)$ through $s_7(t)$, $s_8(t)$ through $s_{11}(t)$, and $s_{12}(t)$ through $s_{15}(t)$. Hypothetically, if one were to form the average of the waveforms in each group (see Fig. 6), i.e.,

[7] Since our interest in this article is focused on improving the power efficiency of the scheme, we shall not pursue the distinction between FQPSK and enhanced FQPSK since, as shown in [13], the two schemes have the same SNR behavior (as measured by minimum squared Euclidean distance).

[8] The necessity of a bias associated with the matched filters comes about because of the fact that the members of the M-ary signaling set defined in Eq. (3) do not all have equal energy.

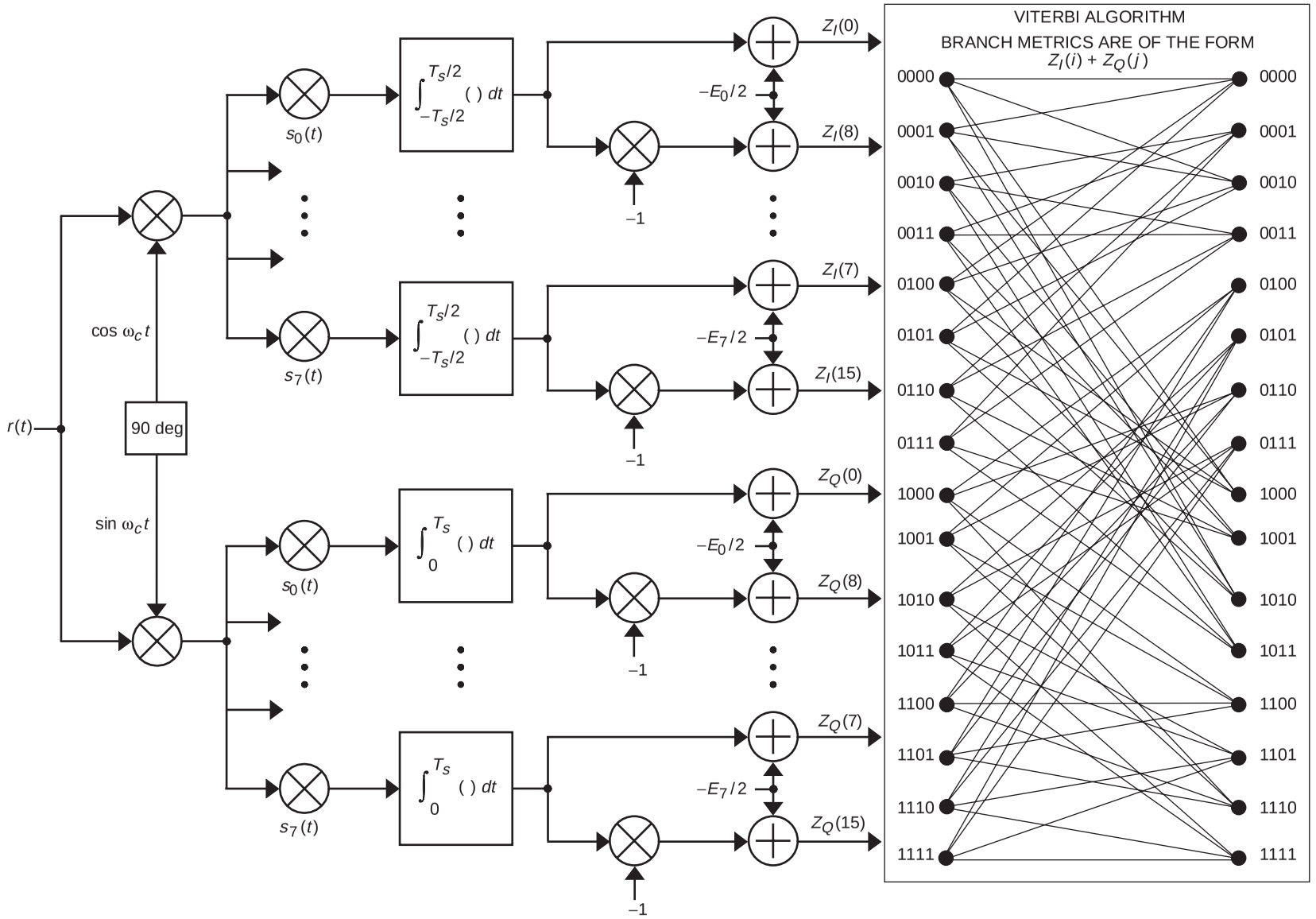

Fig. 4. The optimum trellis-coded receiver for FQPSK.

$$\left.\begin{aligned} q_0(t) &= \sum_{i=0}^{3} s_i(t) \\ q_1(t) &= \sum_{i=4}^{7} s_i(t) \\ q_2(t) &= \sum_{i=8}^{11} s_i(t) = -q_0(t) \\ q_3(t) &= \sum_{i=12}^{15} s_i(t) = -q_1(t) \end{aligned}\right\} \tag{4}$$

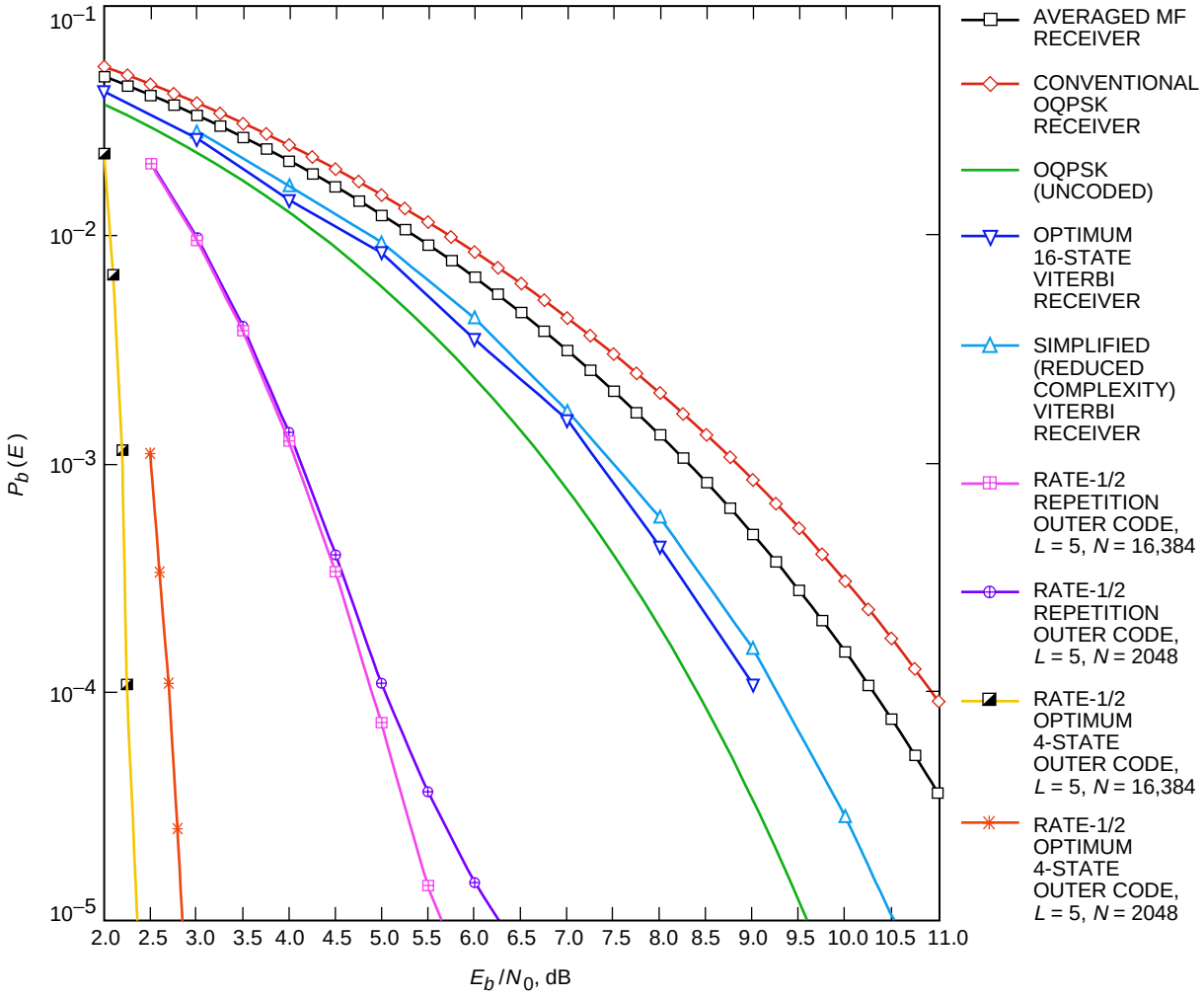

Fig. 5. A comparison of the BER performances of various uncoded and coded FQPSK systems.

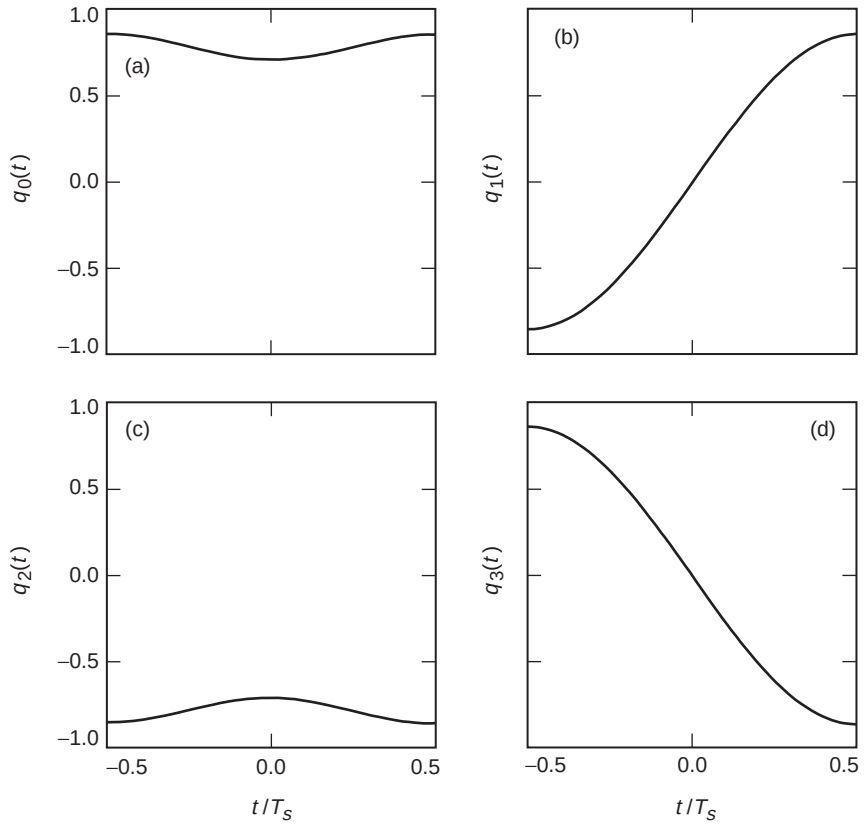

Fig. 6. Averaged waveforms for the simplified Viterbi receiver: (a) $q_0(t)$, (b) $q_1(t)$, (c) $q_2(t)$, and (d) $q_3(t)$, .

and replace the waveform assignments of the group members in Fig. 3 by their corresponding average waveform, e.g., $s_0(t), s_1(t), s_2(t), s_3(t)$ all now become $q_0(t)$; $s_4(t), s_5(t), s_6(t), s_7(t)$ all now become $q_1(t)$, etc., then, because of the relation between the I and Q coded bits and the BCD mapping in Fig. 2, the cross-correlation between the I and Q channels would disappear. To see how this comes about, we note that what ordinarily distinguishes the four waveforms in each group from each other are the two least-significant bits, namely, I_0, I_1 and Q_0, Q_1. Since by sending only one waveform per group, i.e., $q_0(t), q_1(t), q_2(t)$, or $q_3(t)$, we no longer need to make this distinction, then the BCD mapper requires only the two most-significant bits, i.e., I_2, I_3 and Q_2, Q_3, to specify the transmitted waveform pair. By inspection of Fig. 2, we see that this is tantamount to the I-channel signal being chosen based on only the I-encoder output bits and the Q-channel signal being chosen based on only the Q-encoder output bits, i.e., the cross-correlation of the encoder outputs in choosing the I and Q waveforms disappears. Assuming this to be the case, then the trellis-coded structure of the modulation decouples into two independent I and Q 2-state trellises (see Fig. 7), whereupon the transmitter simplifies to the structure in Fig. 8 with the corresponding optimum receiver as in Fig. 9. (We have relabeled the I and Q pairs of bits with a prime notation so that for convenience of notation we can continue to index the transmitted signals between 0 and 4). By independent we mean that the I and Q decisions are no longer produced jointly but rather separately by individual Viterbi algorithms (VAs) acting on the energy-biased correlations derived from the I- and Q-demodulated signals, respectively. This trellis structure of the simplified Viterbi receiver as well as the simplified transmitter of Fig. 8 are identical to that of so-called trellis-coded OQPSK discussed in [16] but with a different waveform assignment. The metrics used for the simplified Viterbi receiver in Fig. 9 are the same as those for the full-blown receiver of Fig. 3 except that the matched-filter biases are now computed from the energies of the waveform averages in Eq. (4) rather than from the energies of the individual waveforms of Eq. (3). Finally, since the true trellis-coded structure of FQPSK entails

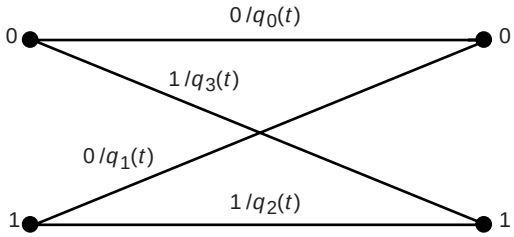

Fig. 7. Trellis diagram for the simplified FQPSK Viterbi receiver.

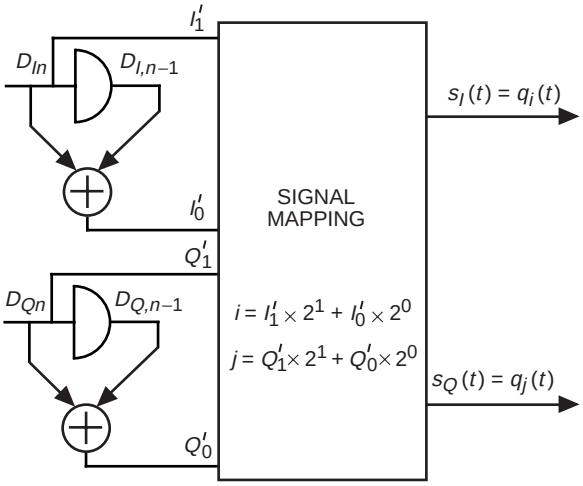

Fig. 8. Simplified implementation of "FQPSK" baseband signals.

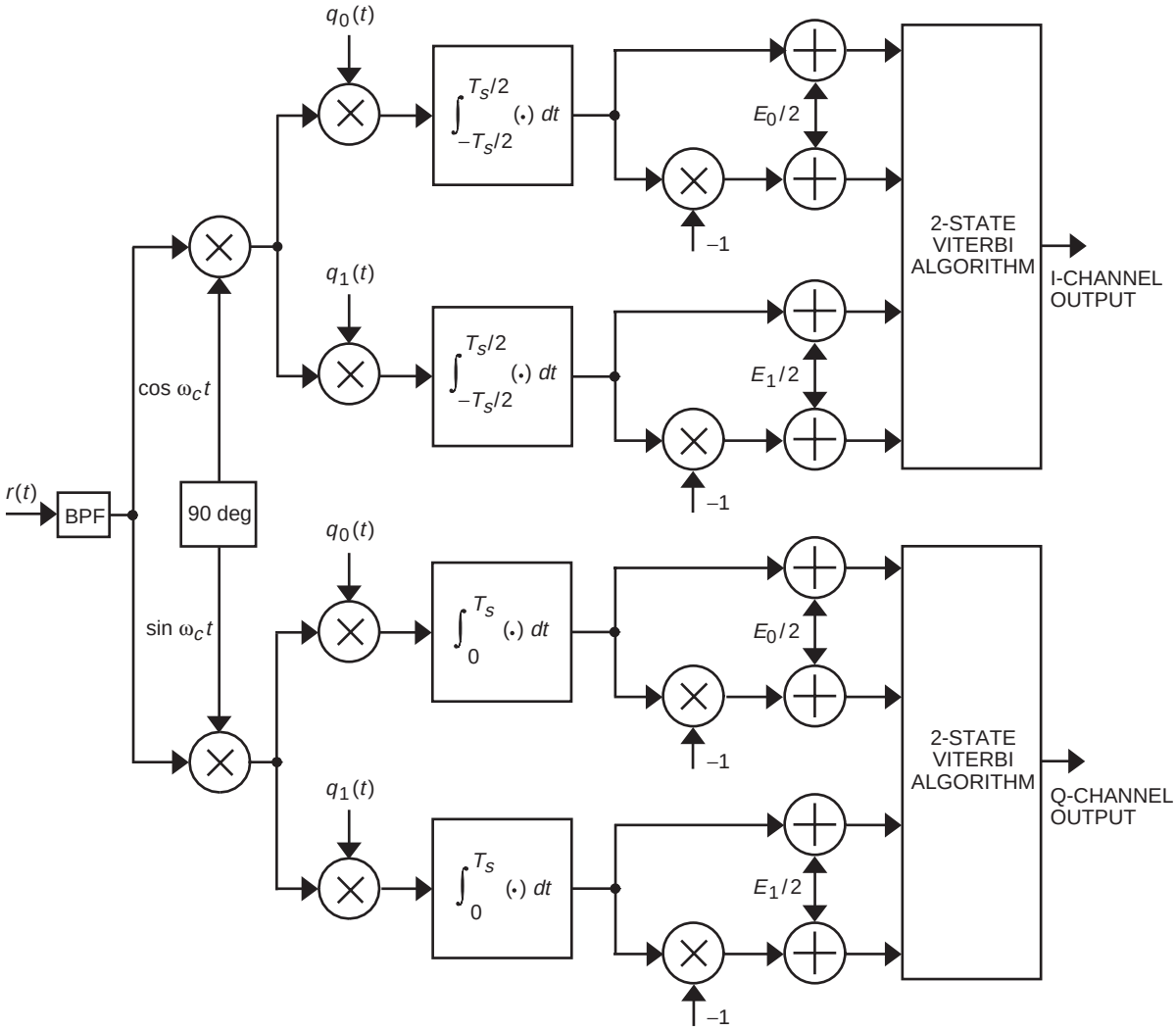

Fig. 9. The simplified FQPSK-B Viterbi receiver.

transmitting a set of 16 different waveforms [as described in Eq. (3)], using the above simplified receiver, which is based on the hypothetical mapping to only the four signals in Eq. (4), for demodulating FQPSK represents a mismatched condition and as such is suboptimum.

Using Signal Processing WorkSystem (SPW) computer simulations, the BER performance of FQPSK using the simplified Viterbi receiver is superimposed here on the results in Fig. 5. Where for the full-blown 16-state Viterbi receiver the truncation path length (decoding depth) was chosen equal to 50 bits, for the simplified receiver a truncation path length of only 10 bits is needed, thereby significantly reducing the decoding delay. Comparing the simplified Viterbi receiver performance with that of the full-blown receiver, the E_b/N_0 loss was 0.25 dB at a BER of 10^{-3} and 0.3 dB at a BER of 10^{-5}. These small degradations are greatly compensated for by the significant reduction in receiver complexity.

III. Error-Correction-Coded FQPSK with Iterative Decoding

Motivated by the potentially large coding gain achievable with iterative decoding of concatenated codes using a soft input–soft output (SISO) a posteriori probability (APP) algorithm, the authors set out to apply this technique to FQPSK, which by virtue of its inherent coding supplies the inner code. To keep matters simple, the investigations considered applying the outer code to an FQPSK system using the simplified receiver of Fig. 9, where the 2-state VAs are now replaced with 2-state SISO algorithms [17] that in a max-log version are equivalent to modified soft-output VAs (SOVAs) [18]. In order to have a coding gain resulting from the interleaving process between the inner and outer codes, we must first remap the I and Q FQPSK nonrecursive inner codes to recursive types [19]. The particular remapping of the input bits and trellis code states of the I and Q inner codes to change the input–output relation required by the concatenated coding scheme is shown in Figs. 10 and 11, respectively. This remapping is aimed at providing recursiveness for the parts of the FQPSK encoders that are matched to the reduced 2-state SISO decoder for the inner code.[9] Furthermore, such a remapping method will provide improved coding gain for the concatenated coded FQPSK system.

It is important to note that, with the remapped encoders of Figs. 10 and 11, in the absence of an outer code, a particular random input bit sequence will now result in a different pair of transmitted I and Q baseband waveforms. However, since the remapping does not change the allowable FQPSK encoder output sequences, the envelope and spectral characteristics of the resulting modulated signal would be identical to the FQPSK signal produced by the transmitter of Fig. 2. If now in the presence of the outer code we assume that the interleaver size is sufficiently large that the random interleaver approximately outputs a random uncorrelated sequence, then the same conclusion regarding the envelope and spectral properties of the transmitted signal in the concatenated coding case once again applies. For example, it is known that, for many optimum convolutional codes (used here as an outer code), a random input bit sequence produces an uncorrelated output sequence.

With regard to the manner in which the outer code is applied to the FQPSK modulator/demodulator, we propose three different concatenation schemes, each of which incorporates iterative decoding. The transmitter–receiver combinations for each of these schemes are illustrated in Figs. 12(a) through 12(c). As in Fig. 9, the energy-biased matched filter bank provides the four required branch metrics (per I and Q channel) for the simplified 2-state SISO FQPSK decoders. The FQPSK SISO decoders in turn provide extrinsics (added-value reliabilities) associated with the FQPSK encoder input bits to the outer decoders through deinterleaver(s). The SISO output decoder(s) provide enhanced versions of the received extrinsics using the code constraint as output extrinsics, which through interleaver(s) are fed back to the inputs of the SISO FQPSK decoders. This process repeats (iterates) several times. At the end of the last iteration,

[9] To see this, note that if once again one were to postulate a hypothetical modulation scheme with a mapping to the signals in Eq. (4), then the encoders of Figs. 10 and 11 would simplify in an analogous manner to the way in which the encoders of Fig. 2 simplified to those in Fig. 8, and the associated 2-state trellis would appear as in Fig. 7 with the input bits on the two transitions emanating from the "1" state reversed.

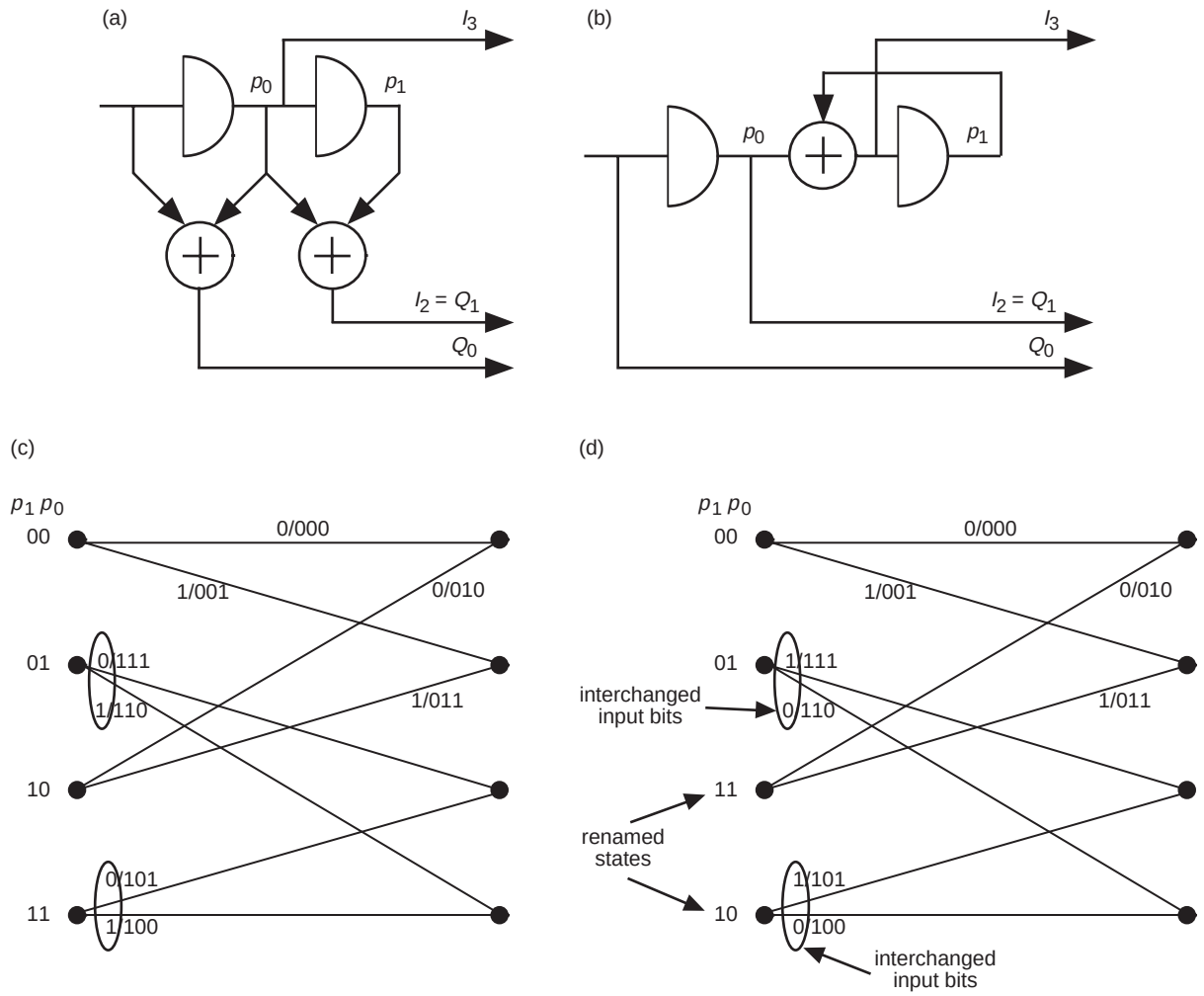

Fig. 10. The I encoder and trellis: (a) original I encoder, (b) remapped I encoder, (c) original I encoder trellis, and (d) remapped I encoder trellis.

the outputs of the SISO outer decoders that correspond to the input bits to the outer encoders are hard-limited to produce decisions on these bits. To reduce the complexity of the SISOs for both the FQPSK decoders and the outer decoders, we simulated max-log versions of these SISOs that, as previously stated, are equivalent to modified versions of the original SOVA proposed by Hagenauer and Hoeher [20].

As a start, the concatenated coding scheme of Fig. 12(a) was used with a simple rate-1/2 repetition outer code followed by a block interleaver of size N applied to the Q-channel encoder and, for simplicity of implementation, no outer code and interleaver applied to the I-channel encoder.[10] At the receiver, the Q-channel 2-state SISO max-log FQPSK decoder generates the soft-output extrinsics required for iterative decoding. These soft-output extrinsics, after being deinterleaved, are provided to the SISO max-log outer decoder, which for a repetition code consists of simply swapping the order of successive pairs of bits (see Fig. 13). The average BER of the Q-channel data was then determined by computer simulation. Since

[10] Since, as we shall see momentarily, the receiver corresponding to this scenario was simulated to measure only BER on the Q channel, because of the previously discussed reasoning that resulted in the independence of the I and Q trellises in Fig. 8, outer coding on the I channel would result in no additional coding gain. However, to match the increase in the symbol rate on the Q channel caused by the inclusion of a rate-1/2 repeat code, the symbol rate on the I channel was also doubled.

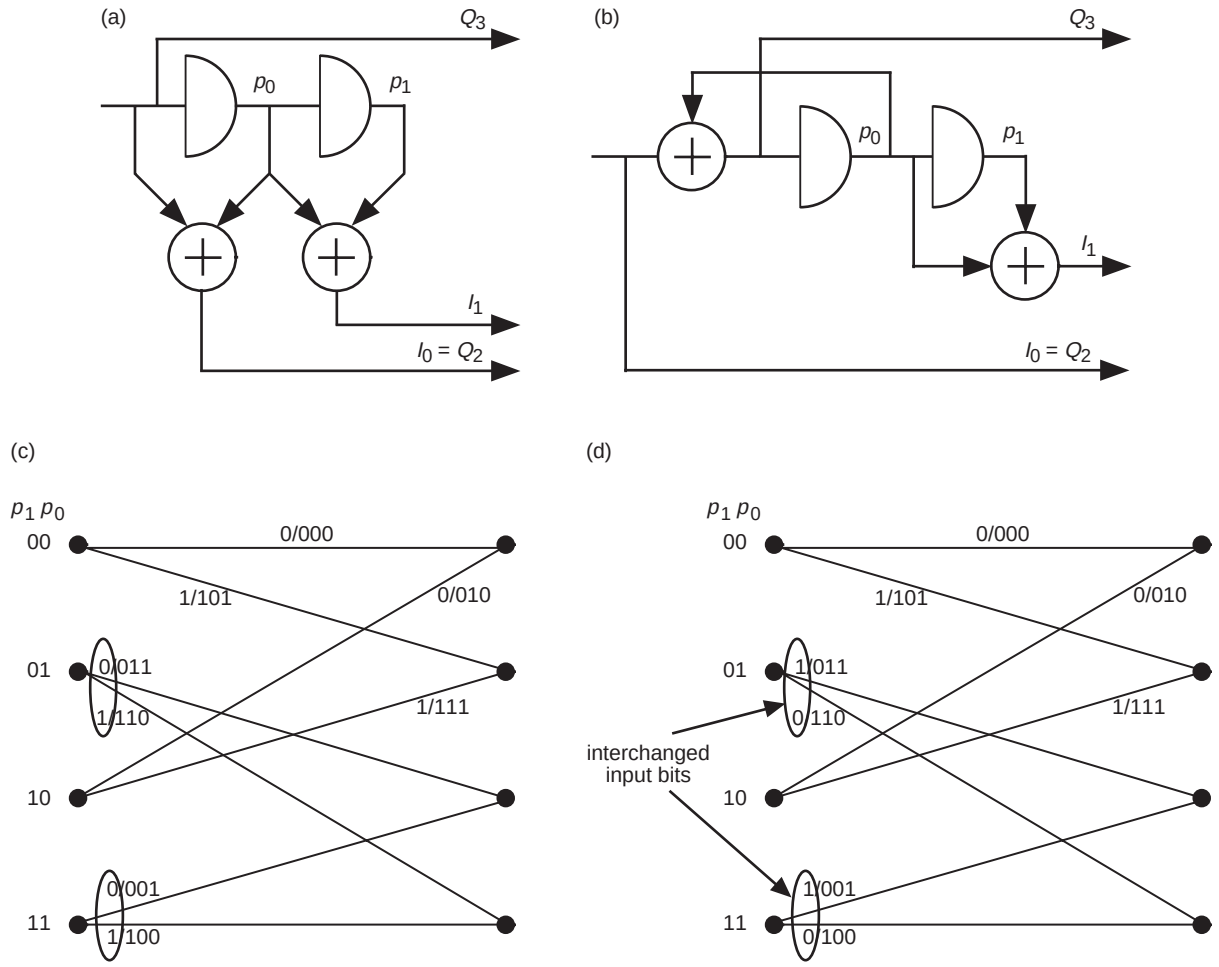

Fig. 11. The Q encoder and trellis: (a) original Q encoder, (b) remapped Q encoder, (c) original Q encoder trellis, and (d) remapped Q encoder trellis.

the rate-1/2 repetition code after sufficiently large interleaving looks like a random data sequence at twice the data rate, then in so far as the output of the FQPSK modulator is concerned, it has the appearance of an FPQSK signal but with twice the bandwidth.

Superimposed on the results in Fig. 5 is the BER performance of the above concatenated coding scheme with $L = 5$ iterations and interleaver block sizes of $N = 2048$ and $N = 16,384$ bits. Using the same rate-1/2 repetition code, similar performance would be expected from the concatenating coding schemes in Figs. 12(b) and 12 (c). We observe from these results that, even with such a very simple outer code, at a BER of 10^{-5} an improvement of 3.75 dB relative to the performance of the simplified FQPSK receiver without outer coding is obtained for $N = 2048$, whereas $N = 16,384$ yields an improvement of 4.5 dB.

The next case considered was a rate-1/2 optimum 4-state outer code with minimum free distance $d_f = 5$. The interleaving gain for this case is asymptotically proportional to N^{-3} versus N^{-1} for the previous case as in turbo codes. The BER performance of this case is also illustrated in Fig. 5 for $L = 5$ iterations and interleaver block sizes of $N = 2048$ and $N = 16,384$ bits. At the same BER of 10^{-5}, the improvement relative to that of the simplified FQPSK receiver without outer coding has now increased to 7.25 dB for $N = 2048$ and 7.7 dB for $N = 16,384$.

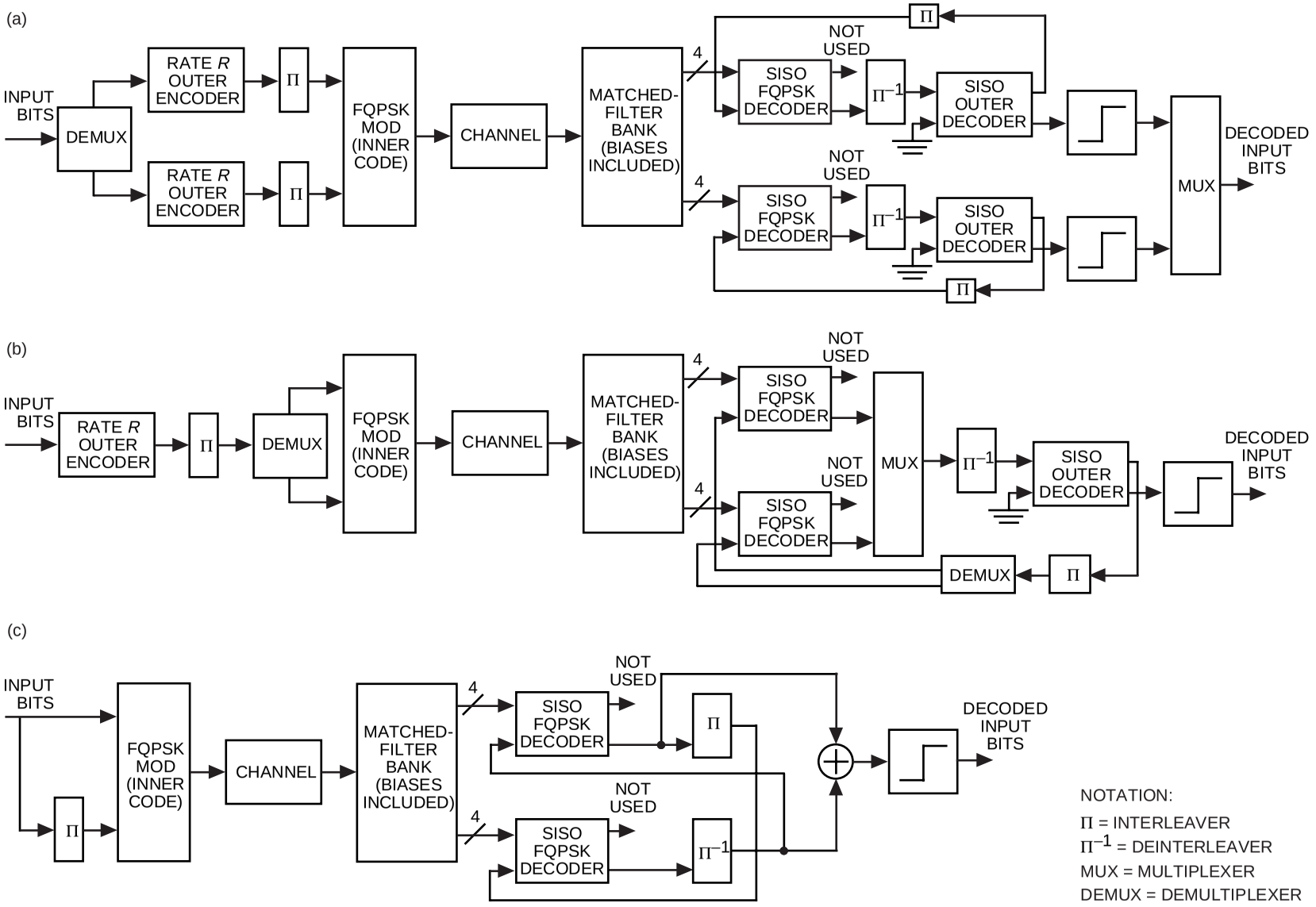

Fig. 12. Several transmitter–receiver combinations for coded FQPSK with iterative decoding: (a) serial concatenation scheme 1, (b) serial concatenation scheme 2, and (c) parallel concatenation scheme.

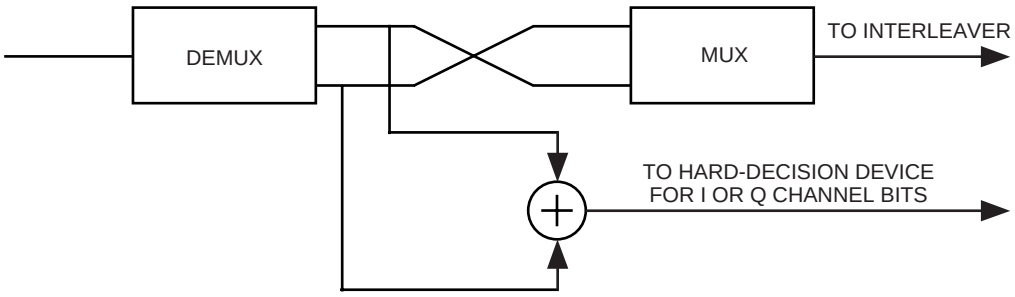

Fig. 13. SISO outer decoder for rate-1/2 repetition code.

IV. Conclusions

We have shown that, by applying simple (a small number of states) outer codes to a FQPSK modulation to form a concatenated coding arrangement with iterative decoding, it is possible to achieve a highly power- and bandwidth-efficient system. Several possible configurations for the concatenation were suggested, and specific numerical results were presented for one of these in order to demonstrate the large coding gains that are potentially achievable even when using a reduced-complexity FQPSK receiver. In view of the very positive results reported here, further investigation of the other concatenated coding schemes is warranted as well as consideration of higher-rate codes to reduce the bandwidth expansion proportional to the inverse of the code rate.

References

[1] K. Feher et al., U.S. Patents 4,567,602; 4,339,724; 4,644,565; 5,784,402; 5,491,457. Canadian Patents 1,211,517; 1,130,871; 1,265,851.

[2] K. Feher, *Wireless Digital Communications: Modulation and Spread Spectrum Applications*, Upper Saddle River, New Jersey: Prentice Hall, 1995.

[3] K. Feher, *Digital Communications: Satellite/Earth Station Engineering*, Littleton, Colorado: Crestone Engineering, 1996.

[4] K. Feher, "F-QPSK—A Superior Modulation Technique for Mobile and Personal Communications," *IEEE Transactions on Broadcasting*, vol. 39, no. 2, pp. 288–294, June 1993.

[5] K. Feher, "FQPSK Transceivers Double the Spectral Efficiency of Wireless and Telemetry Systems," *Applied Microwave and Wireless*, vol. 10, no. 6, June 1998; also presented at European Telemetry Conference, ETC '98, Garmish-Patternk, Germany, May 5–8, 1998.

[6] S. Kato and K. Feher, "XPSK: A New Cross-Correlated Phase-Shift-Keying Modulation Technique," *IEEE Transactions on Communications*, vol. 31, no. 5, pp. 701–707, May 1983.

[7] M. C. Austin and M. V. Chang, "Quadrature Overlapped Raised-Cosine Modulation," *IEEE Transactions on Communications*, vol. 29, no. 3, pp. 237–249, March 1981.

[8] W. L. Martin, T.-Y. Yan, and L. V. Lam, "CCSDS-SFCG: Efficient Modulation Methods Study at NASA/JPL, Phase 3: End-to-End Performance," SFCG Meeting, Galveston, Texas, September 1997.

[9] K. Murota, K. Kinoshita, and K. Hirade, "Spectrum Efficiency of GMSK Land Mobile Radio," ICC'81 Conference Record, Denver, Colorado, pp. 23.8.1–23.8.5, June 14–18, 1981.

[10] M. R. L. Hodges, "The GSM Radio Interface," *British Telecom Technological Journal*, vol. 8, no. 2, January 1990.

[11] *IRIG Telemetry Standard 106-00*, Secretariat of Range Commanders Council, U.S. Army, White Sands, New Mexico, January 2000.

[12] M. K. Simon and T.-Y. Yan, "Cross-Correlated Trellis Coded Quadrature Modulation," patent filed October 5, 1999.

[13] M. K. Simon and T.-Y. Yan, "Unfiltered Feher-Patented Quadrature Phase-Shift-Keying (FQPSK): Another Interpretation and Further Enhancements: Parts 1, 2," *Applied Microwave & Wireless Magazine*, vol. 12, no. 2/no. 3, pp. 76–96/pp. 100–105, February/March 2000.

[14] D. Lee, M. K. Simon, and T.-Y. Yan, "Enhanced Performance of FQPSK-B Receiver Based on Trellis-Coded Viterbi Demodulation," ITC '00, San Diego, California, October 23–26, 2000.

[15] T. Le-Ngoc, K. Feher, and H. Pham Van, "New Modulation Techniques for Low-Cost Power and Bandwidth Efficient Satellite Earth Stations," *IEEE Transactions on Communications*, vol. 30, no. 1, pp. 275–283, January 1982.

[16] M. K. Simon, P. Arabshahi, and M. Srinivasan, "Trellis-Coded Quadrature-Phase-Shift Keying (QPSK) With Variable Overlapped Raised-Cosine Pulse Shaping," *The Telecommunications and Mission Operations Progress Report 42-136, October–December 1998*, Jet Propulsion Laboratory, Pasadena, California, pp. 1–16, February 15, 1999.
http://tmo.jpl.nasa.gov/tmo/progress_report/42-136/136F.pdf

[17] S. Benedetto, D. Divsalar, G. Montorsi, and F. Pollara, "Soft-Input Soft-Output Modules for the Construction and Distributed Iterative Decoding of Code Networks," *European Transactions on Telecommunications*, vol. 9, no. 2, pp. 155–172, March–April 1998.

[18] M. P. C. Fossorier, F. Burkert, S. Lin, and J. Hagenauer, "On the Equivalence Between SOVA and Max-Log-MAP Decodings," *IEEE Communications Letters*, vol. 2, no. 5, pp. 137–139, May 1998.

[19] S. Benedetto, D. Divsalar, G. Montorsi, and F. Pollara, "Serial Concatenation of Interleaved Codes: Performance Analysis, Design, and Iterative Decoding," *IEEE Transactions on Information Theory*, vol. 44, no. 3, pp. 909–926, May 1998.

[20] J. Hagenauer and P. Hoeher, "A Viterbi Algorithm with Soft-Decision Outputs and Its Application," *GLOBECOM '89 Proceedings*, vol. 3, Dallas, Texas, pp. 43.3.1–43.3.5, November 1989.